HIGH-CURRENT ZINC-AIR MICROBATTERY BASED ON A MICROMACHINED MULTILAYER LATERAL METALLIC SCAFFOLD

A. Armutlulu[1*], Y. Fang[1], S.-H. Kim[2], C.-H. Ji[2], S. A. B. Allen[1], and M. G. Allen[1,2]
[1]School of Chemical and Biomolecular Engineering, Georgia Institute of Technology, Atlanta, USA
[2]School of Electrical and Computer Engineering, Georgia Institute of Technology, Atlanta, USA
*Presenting Author: aarmutlulu3@gatech.edu

Abstract: We present a three-dimensional zinc-air microbattery with improved discharge rate and reduced internal resistance. The device is based on a multilayer, micron-scale, high surface area metallic scaffold 'skeleton'. This scaffold consists of alternating copper and nickel layers supporting zinc as electrodeposited anode material. A proof-of-concept zinc-air microbattery based on this technology was developed, characterized, and compared with commercially available zinc-air batteries. A single layer initial structure with a surface area of 0.9 mm^2 has been improved to a scaffold structure with 10 layers having a surface area of 10 mm^2. The areal energy density of the microbattery was measured as 1.5~3 mWh/cm^2 under discharging through resistances ranging from 540 to 5000 Ω.

Keywords: zinc-air microbattery, robotic electroplating, high aspect-ratio, multilayer metallic scaffold

INTRODUCTION

Even though there has been enormous progress in the development of microdevices, encompassing autonomous microactuators as well as microsensors for ubiquitous sensor networks (USNs) and for implantable microsystems, the development of compatible and suitably-sized power sources remains elusive. Batteries utilize mature electrochemistry and provide sufficient voltage for microelectronics with a relatively high energy density. In order to maximize the performance of the batteries in microdevices with limited available area, or small footprints, microbatteries with three-dimensional (3D) architecture as opposed to two-dimensional (2D) thin-film battery electrodes are needed which incorporate high aspect ratio electrode structures for maximum surface area, and accordingly maximum energy density [1].

Zinc-air batteries are good candidates for the previously mentioned microscale applications due to both their high energy densities and their use of atmospheric oxygen as the cathode reactant. Commercial zinc-air batteries utilize Zn powder for the anode, achieving high surface area as well as high energy density [2]. However, zinc oxide formation on the anode over time results in an increase in the internal resistance which limits the discharge rate of the battery and thus decreases its performance [3]. In order to maintain the inherent high energy density and improve the discharge characteristics of the zinc-air battery, microfabricated zinc-air batteries with well-ordered 3D Zn pillar microstructures for high surface area and reduced internal resistance have been demonstrated [3,4].

While the reported research addresses performance improvement in the zinc-air microbattery by increasing the aspect ratio of the 3D Zn electrodes, this paper focuses on the development of 3D Zn anode structures coated on highly-laminated metallic skeletons, based on a robotic electroplating process [5]. The mechanically firm and conductive metallic skeleton with submicron thick multilayers not only provides high surface area enabling high discharge rates, but also enables controlled and consistent electrical access to the Zn anode for improved discharge characteristics.

EXPERIMENTAL

Fabrication of the Zn anode

The fabrication process of the Zn anode is schematically demonstrated in Fig. 1. A Ti/Cu/Ti seed layer was sputtered onto thermally oxidized silicon wafer. The seed layer was coated with a 100 µm thick photoresist layer. Negative tone photoresists such as SU-8 2025 (Microchem) or NR21 (Futurrex) have been used to create desired patterns to be utilized as a high aspect ratio electroplating mold for the metallic skeleton structures with 50 layers. For the structures with 10 layers, NR-21 is preferred due to its simplicity in removal after electroplating.

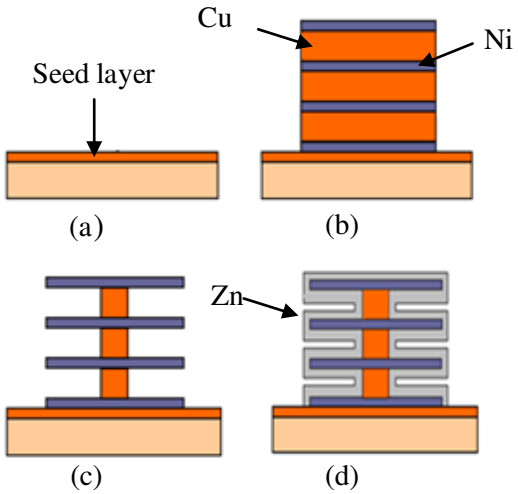

Fig. 1: Schematic of the fabrication process for the Zn anode structure: (a) sputter deposition of Ti-Cu-Ti seed layer, (b) electrodeposition of alternating Ni and Cu layers, (c) selectively etching Cu layers to build the skeleton, (d) electrodeposition of Zn onto the skeleton.

The next step involves the scaffold building process which is based on sequential robotic electroplating [5]. After the removal of the top Ti seed layer by diluted HF, multilayers of Ni and Cu were alternately electroplated at a constant current density of 10 mA/cm^2. Both Ni and Cu layers have been plated from their respective sulfate based baths [6].

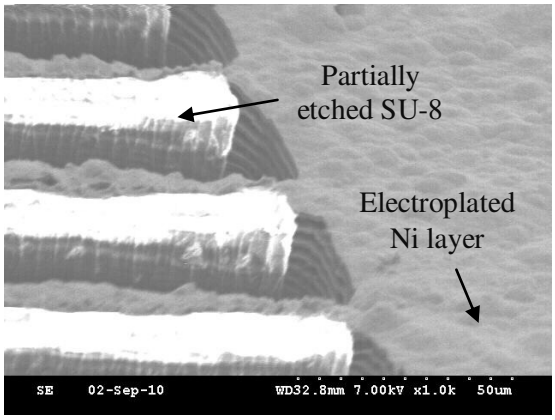

Fig. 2: Scanning electron microscope (SEM) image of the Ni scaffold. SU-8 mold has been partially removed by oxygen plasma RIE: magnified view of the inner walls of the metallic skeleton.

The removal of the SU-8 mold by plasma reactive-ion etching (RIE) process was followed by selective chemical etching of the Cu layers to give the final shape of the Ni skeleton. In the case of NR21 negative photoresist, acetone/methanol treatment has been used to remove the mold. Although it is difficult to remove the SU-8 mold completely using the RIE and thus residues remained inside the holes of the metallic skeleton, a significant gap has been formed between the mold and the skeleton such that the Cu etchant solution could diffuse in and selectively etch the Cu layers. This can be clearly seen in Fig. 2 where the SEM image of the Ni scaffold is depicted after selective Cu etching and before Zn electrodeposition.

In order to etch the Cu layers selectively, a solution of ammonium hydroxide saturated with copper sulfate has been utilized. The experimentally determined etching rate was found to be approximately 0.6 μm per minute. Estimating the Cu etching rate is a rather crucial step since it plays a key role in increasing the surface area of the structure. The more Cu is etched, the more surface area is exposed to be electroplated. On the other hand, it is also important to preserve certain amount of Cu in order to provide both mechanical support and electrical connection between the Ni layers.

Two different mesh patterns that have been used to build the test samples are given in Fig. 3. In Fig. 3 (a), dark regions on the patterns represent etch-holes which are vertically 15 μm apart from each other. All the Cu between vertically adjacent etch holes has been completely etched away. This way, the Ni air-bridges have been formed and all the mechanical support, as well as the electrical connection, have been provided by the Cu remained between the columns of the etch-holes. Therefore, it is crucial to determine the optimum etching time in order to prevent an under-etching which significantly inhibits the surface area increase, or an over-etching which causes the Ni layers to be delaminated.

Two proof-of-concept 10-layer Ni scaffold structures have been built based on both square and rectangular patterns. For a given etching time period, the structure built on the square pattern shown in Fig. 3(a) has a surface area that is more than 4 times greater than its footprint area whereas the rectangular pattern based structure in Fig. 3(b) yields less than 2-fold increase. In terms of surface area, on the other hand, the increase for the former structure turns out to be more than 10 fold. In theory, it is possible to dramatically increase the surface area by using more complex 2D mesh-like metallic patterns and by increasing the number of layers [5].

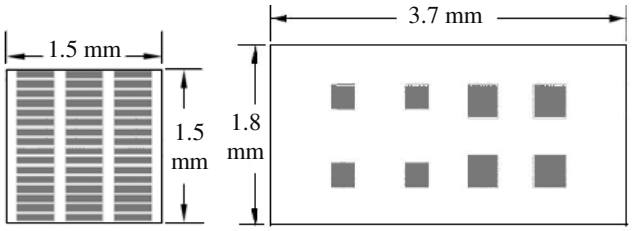

Fig. 3: Two different mesh patterns used to build the metallic skeleton. Dark areas refer to the etch-holes covered with photoresist mold during the Ni and Cu electroplating process.

The final step of the Zn anode fabrication process involves electrodeposition of Zn onto the Ni skeleton. Zn was electroplated at a constant current density of 10 mA/cm^2 utilizing an acid chloride Zn electroplating bath [6]. The SEM image of the anode after the Zn electrodeposition process is shown in Fig. 4.

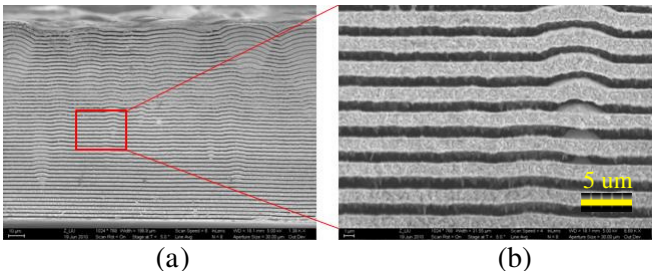

Fig. 4: SEM images of the side views of the Zn anode before discharge test: (a) sidewall of the 50-layer skeleton structure after Zn electroplating, (b) enlarged image showing *the 1.4 μm thick Zn* coated layers.

Assembly of the zinc-air microbattery

Fig. 5 depicts the schematic of the final form of the zinc-air battery. The fabricated anode structure was assembled with a commercially available air cathode (E4A with separator, Electric Fuel Limited). This air cathode consists of three major layers [7]. The top

blocking layer made of laminated porous Teflon film allows oxygen to diffuse in and prevents the battery from leaking electrolyte. The active layer is located in the middle and contains manganese based catalyzed carbon as the active material supported by a woven Ni mesh. To complete the circuit in the testing stage, a copper wire is soldered to the edge of this Ni mesh after cleaning off the carbon. The very bottom layer facing the electrolyte is called separator layer which is a laminate of a polypropylene microporous film with a thin polypropylene non-woven that is made hydrophilic with a surfactant. It acts as an insulator between the anode and cathode while allowing flow of ions in the electrolyte. The cut edges of the air cathode were sealed with epoxy.

7M aqueous KOH solution to be used as the electrolyte was injected into the assembled microbattery following a vacuum treatment. The vacuum treatment ensures the removal of the air trapped deep in between the laminated layers and thus provides a perfect contact between the electrolyte and the whole Zn anode surface.

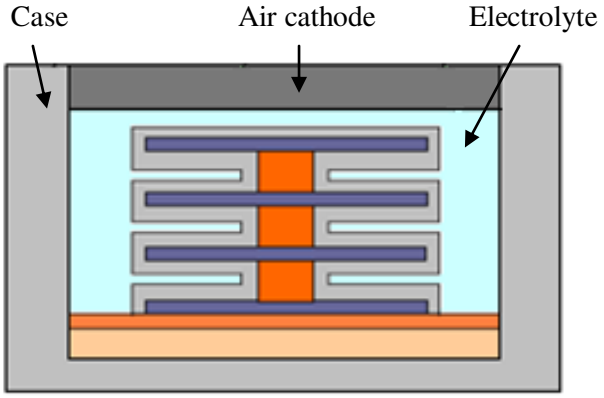

Fig. 5: Schematic of the encapsulated Zn anode with an air cathode and KOH electrolyte.

Performance tests

The 10-layer and 50-layer sample batteries were tested by discharging under four different electrical loads. These four electrical loads used in the tests had the resistance values of 540, 1000, 3000, and 5000 Ω. During the discharge tests, voltage values were measured and recorded with respect to time by using a software tool (LabVIEW SignalExpress). Fig. 6 shows the SEM image of the 50-layer zinc-air battery before and after the discharge test.

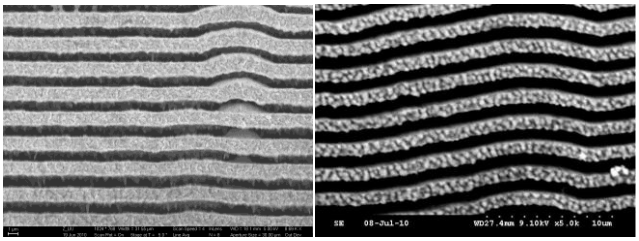

(a) (b)

Fig. 6: SEM image showing the side wall of the 50-layer Zn anode after discharge tests: (a) before discharge (b) after discharge.

RESULTS AND DISCUSSION

Discharge characteristics of the fabricated zinc-air microbatteries under different electrical loads are illustrated in Fig. 7. The discharge curves maintain relatively flat voltage profiles over time, with a small voltage decrease right after the start-up, and a sharp voltage decrease near total discharge.

These discharge data were also used to calculate the areal energy density E of the battery which was determined to be in the range of 1.5-3 mWh/cm^2 at the given four discharge rates. To determine the areal energy density of the zinc-air battery, firstly, its capacity Q in miliampere-hours was calculated by taking the integral of the discharge current I_d over time t. The capacity was then multiplied by the average discharge voltage V_{av} and divided by the footprint area A to give areal energy density.

$$Q = \int I_d dt \quad (1)$$

$$E = \frac{Q \cdot V_{av}}{A} \quad (2)$$

The calculated areal energy densities for a sample with 10 layers and 1.5x1.5 mm^2 footprint area, as well as with 50 layers and 3.7x1.8 mm^2 footprint area are summarized in Fig. 8. Since the latter one was built on a larger area, it possesses a relatively lower areal energy density. As opposed to their commercial counterparts, the energy densities of the zinc-air microbatteries do not show any decreasing trend with discharge rate [7]. In fact, a slight increase in the areal energy density can be observed as the discharge rate increases, which indicates that the internal resistance is not significantly affected by the discharge rate.

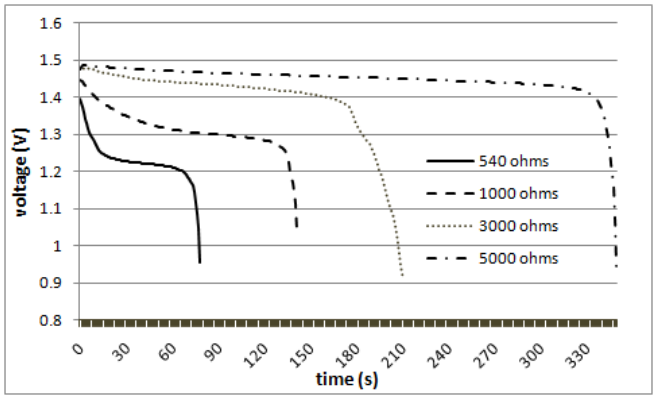

Fig. 7: Discharge characteristics of the 10-layer zinc-air microbatteries under four different electrical loads.

The initial voltage of the fabricated zinc-air microbattery was measured along with that of a commercial zinc-air battery (Duracell DA10) under three different electrical loads. These data for both batteries were compared in Fig. 9. The same trend as in Fig. 9 also persists in the operating voltage over time. The operating voltage of the commercial zinc-air batteries is typically around 1.25 V [2]. The zinc-air microbatteries proposed in this work, however, can

operate at values as high as 1.45 V. The relatively higher voltage values of the fabricated zinc-air microbatteries suggest that they might have lower internal resistance compared to their commercial counterpart and thus allow higher discharge rates. This is currently being investigated.

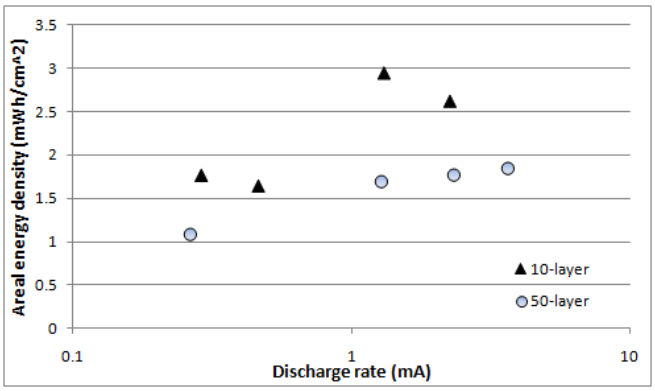

Fig. 8: Areal energy densities of both 10-layer and 50-layer zinc-air microbatteries at four different discharge rates.

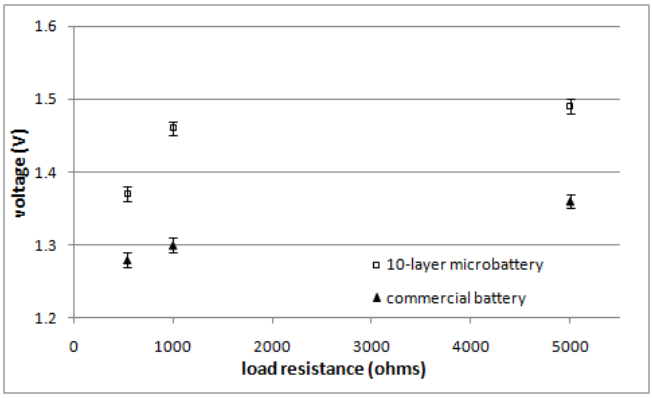

Fig. 9: Initial voltage variation with respect to load resistance for 10-layer and commercial zinc-air batteries.

CONCLUSION

The design, fabrication process, and testing of a proof-of-concept 3D zinc-air microbattery based on a micromachined metallic lateral scaffold supporting electrodeposited Zn anode material with an improved discharge rate and a reduced internal resistance have been discussed. Test results supported the fact that the zinc-air microbattery is capable of providing high discharge rates. In addition, a comparison with commercial zinc-air batteries showed that a lower internal resistance might be achievable with this technology.

ACKNOWLEDGEMENT

The authors would like to thank William Preston Galle, Richard Shafer, and Zhan Liu for their help on the electroplating robot, battery characterization, and high resolution SEM images, respectively.

REFERENCES

[1] Harb J N, LaFollette R M, Selfridge R H, Howell L L 2002 Microbatteries for self-sustained hybrid micropower supplies, J. Power Sources **104** 46-51

[2] http://www.duracell.com, Webpage accessed in July, 2010

[3] Chamran F, Min H S, Dunn B, Kim C J 2007 Zinc-air Microbattery Electrode Array of Zinc Microposts, Proc. IEEE Int. Conf. MEMS 2007 (Kobe, Japan, 21-25 January) 871-874

[4] Dunn B, Long J W, Rolison D. R 2008 Rethinking Multifunction in Three Dimensions for Miniaturizing Electrical Energy Storage, ECS Interface **17**(3) 49-53

[5] Galle P, Kim S H, Shah U, Allen M A 2010 Proc. IEEE Int. Conf. MEMS 2010 (Wanchai, Hong Kong, 24-28 January) 332-335

[6] Schlesinger M, Paunovic M, 2000 Modern Electroplating (New York, Wiley)

[7] Linden D, Reddy T, 2001 Handbook of Batteries (New York, McGraw-Hill)